

Transport, magnetic, thermodynamic, and optical properties in Ti-doped Sr₂RuO₄

K. Pucher, J. Hemberger, F. Mayr, V. Fritsch, and A. Loidl

Experimentalphysik V, Elektronische Korrelationen und Magnetismus, Institut für Physik, Universität Augsburg, D-86135 Augsburg, Germany

E.-W. Scheidt

Experimentalphysik III, Institut für Physik, Universität Augsburg, D-86135 Augsburg, Germany

S. Klimm, R. Horny, and S. Horn

Experimentalphysik II, Institut für Physik, Universität Augsburg, D-86135 Augsburg, Germany

S. G. Ebbinghaus and A. Reller

Festkörperchemie, Institut für Physik, Universität Augsburg, D-86135 Augsburg, Germany

R. J. Cava

Department of Chemistry and Princeton Materials Institute, Princeton University, Princeton, New Jersey 08544

(Received 20 July 2001; revised manuscript received 19 October 2001; published 1 March 2002)

We report on electrical resistivity, magnetic susceptibility, and magnetization on heat-capacity and optical experiments in single crystals of Sr₂Ru_{1-x}Ti_xO₄. Samples with $x=0.1$ and 0.2 reveal purely semiconducting resistivity behavior along c and the charge transport is close to localization within the ab plane. A strong anisotropy in the magnetic susceptibility appears at temperatures below 100 K. Moreover magnetic ordering in the c direction with a moment of order $0.01 \mu_B/\text{f.u.}$ occurs at low temperatures. On doping the low-temperature linear term of the heat capacity becomes significantly reduced and probably is dominated by spin fluctuations. Finally, the optical conductivity reveals the anisotropic character of the dc resistance, with the in-plane conductance roughly following a Drude-type behavior and an insulating response along c .

DOI: 10.1103/PhysRevB.65.104523

PACS number(s): 74.70.-b, 74.62.Dh, 75.30.Cr, 75.50.Cc

I. INTRODUCTION

After the synthesis and characterization of Sr₂RuO₄ (Ref. 1) the system gained considerable interest after reports of superconductivity below $T \approx 1$ K by Maeno *et al.*² The extremely strong suppression of superconductivity on nonmagnetic impurities^{3,4} gave hints of unconventional superconductivity. That triplet pairing might be favored in Sr₂RuO₄ was pointed out in early discussions.⁵⁻⁷ And indeed, at present there exists sound experimental evidence that the superconducting order parameter is of p -wave symmetry: NMR Knight shift,⁸ muon spin rotation,⁹ and small-angle scattering from the flux lattice¹⁰ support the idea that the superconducting state breaks time-reversal symmetry, not compatible with either s -wave or d -wave states. Furthermore, power-law dependencies of the heat capacity, $C \propto T^2$ (Refs. 11 and 12), and of the spin-lattice relaxation rate, $1/T_1 \propto T^3$ (Ref. 13), are fingerprints of unconventional superconductivity.

In analogy to ³He, one is tempted to assume that p -wave pairing is mediated via ferromagnetic (FM) spin fluctuations. Indeed, related compounds are dominated by FM interactions: SrRuO₃ becomes ferromagnetic below 160 K (Ref. 14) and Sr₃Ru₂O₇ orders ferromagnetically at 100 K under hydrostatic pressure.¹⁵ However, quite astonishingly there is not much experimental evidence for ferromagnetic spin fluctuations in the pure compound. Incommensurate Fermi-surface nesting and antiferromagnetic (AFM) spin fluctuations have been detected by inelastic neutron scattering.¹⁶ In addition, strongly anisotropic spin fluctuations have been ob-

served in ¹⁷O-NMR experiments^{17,18} with significant AFM character. However, similar NMR results by Imai *et al.*¹⁹ were interpreted to result from orbital-dependent ferromagnetic correlations. The fact that the presence of FM and AFM spin fluctuations yields a strong competition between d - and p -wave superconductivity²⁰ or that spin-triplet superconductivity may even arise from AFM spin fluctuations²¹ has been pointed out theoretically. Doping experiments, aiming to induce long-range magnetic order, seem to be important to unravel the question of the importance of FM vs AFM spin fluctuations in Sr₂RuO₄.

Strontium ruthenate is almost isostructural to the high- T_c parent compound La₂CuO₄. The superconductivity is carried by the RuO₂ layers within strongly hybridized oxygen p and ruthenium d states. As has been pointed out, superconductivity in Sr₂RuO₄ is extremely sensitive to defect states and it is clear that substituting Ru⁴⁺ ($4d^4$) by nonmagnetic Ti⁴⁺ ($3d^0$) will suppress superconductivity. However it seems interesting to check the closeness of the pure system to a magnetically ordered ground state and the nature of the magnetism that can be induced by doping. We recall that Ca₂RuO₄ is an AFM insulator²² while Sr₂IrO₄ is a weakly ferromagnetic insulator.^{23,24} On substituting Ru for Ir, Ru exhibits its full local $S=1$ moment up to a critical concentration, beyond which the local moment disappears.²³ Polycrystalline samples of Sr₂Ru_{1-x}Ti_xO₄ with $0 < x < 1$ have been synthesized by Oswald *et al.*²⁵ and their reduction behavior and room-temperature resistivity have been studied. With increasing Ti content the samples were found to show a higher

TABLE I. Lattice constants for $\text{Sr}_2\text{Ru}_{1-x}\text{Ti}_x\text{O}_4$ at room temperature for $x=0.1$ and 0.2 .

Ti concentration x	Lattice constants in angstrom	
	a, b	c
0	3.8704(1)	12.7435(1)
0.1	3.8744(1)	12.7163(1)
0.2	3.8775(1)	12.7008(2)

resistivity while the tendency to be reduced decreases.

While this paper was in preparation we became aware of similar experiments by Minakata and Maeno²⁶ who investigated the electrical resistivity and the magnetic susceptibility for $\text{Sr}_2\text{Ru}_{1-x}\text{Ti}_x\text{O}_4$ for Ti concentrations $0 < x < 0.25$. These authors found local-moment formation exhibiting strong Ising anisotropy. A magnetic moment of $0.5\mu_B$ per Ti was calculated and the magnetic order has been characterized as spin-glass-like. Here we present measurements of the electrical resistivity, the magnetic susceptibility, the heat capacity, and the optical conductivity of single-crystalline material doped with 10% and 20% Ti. Our results reveal a strong magnetic and electronic anisotropy of the doped compounds. On increasing Ti concentration the resistivity increases and the Sommerfeld coefficient significantly decreases. In addition we find at low temperatures magnetic ordering is induced, whose nature is not fully understood.

II. EXPERIMENTAL DETAILS

Single crystals of $\text{Sr}_2\text{Ru}_{1-x}\text{Ti}_x\text{O}_4$ were grown by the floating-zone melting technique in a CSI FZ-T-10000-H furnace. The polycrystalline starting materials were synthesized by conventional solid state reactions from SrCO_3 , RuO_2 , and TiO_2 . To take into account the evaporation of some RuO_2 during the crystal growth, a 10% excess of ruthenium oxide was used. Rods of the polycrystalline compounds with approximately 7 mm diameter and 100 mm length were pressed and sintered at 1350°C for 24 h. For the crystal growth experiments power lamps of 1500 W each were used. The growth was performed in flowing air (1 l/h) with a growth rate of 5 mm/h. The seed and feed rods were counterrotated at a speed of 35 rpm. The resulting boules consisted of a large number of crystals. We found that these crystals can easily be separated by keeping the boules in air for a few days or by putting them in water for several hours. The single-crystalline samples examined in this work were platelets with typical dimensions of 1–3 mm in the a or b direction and well below 1 mm in the c direction.

For a structural characterization, small pieces of the single crystals were powdered and investigated by x-ray diffraction. The Ti-doped samples reveal the same body-centered tetragonal unit cell and space group ($I4/mmm$) as the pure compounds. The lattice constants are listed in Table I and are in good agreement with earlier published values.^{2,26} On increasing x , the in-plane lattice constants slightly increase while c reveals a slight decrease. However, an uncertainty in the Ti concentration of $\pm 3\%$ cannot be ruled out.

The two principal components ρ_{ab} and ρ_c of the electrical

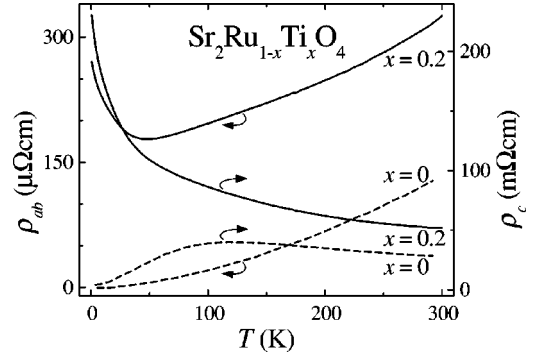


FIG. 1. Temperature dependence of the in-plane resistivity ρ_{ab} (left scale) and interplane ρ_c (right scale) in $\text{Sr}_2\text{Ru}_{0.8}\text{Ti}_{0.2}\text{O}_4$ (solid lines) compared to the undoped compound (dashed lines) (Ref. 29).

resistivity tensor were measured using the Montgomery method²⁷ for temperatures $0.3 \text{ K} < T < 300 \text{ K}$. The specific heat was investigated with noncommercial setups employing relaxational methods²⁸ at low temperatures ($T < 4 \text{ K}$) as well as quasiadiabatic and ac methods at elevated temperatures. The magnetic properties were measured employing a superconducting quantum interference device (Quantum Design MPMS) in a temperature range $1.8 \text{ K} < T < 400 \text{ K}$ and in fields up to 50 kOe.

For the measurements of the optical reflectivity we used two Fourier-transform infrared (IR) spectrometers with full bandwidths of 50 to 8000 cm^{-1} (Bruker IF113v) and 500 to 33000 cm^{-1} (Bruker IFS 66v/S) together with an Oxford Optistat cryostat. The polarization-dependent reflectivity at room temperature was investigated using a Bruker IRscope II microscope, which offers the possibility to investigate small fractions of the sample surface in a range well below 0.1 mm^2 . All IR measurements were carried out on cleaved (not polished) single crystals.

III. RESULTS AND DISCUSSION

A. dc resistivity

The interlayer resistivity, ρ_c , and the in-plane resistivity, ρ_{ab} , were measured for temperatures $0.3 \text{ K} < T < 300 \text{ K}$. As an example Fig. 1 shows the results for $\text{Sr}_2\text{Ru}_{0.8}\text{Ti}_{0.2}\text{O}_4$ (solid lines) compared to the pure compound (dashed lines).² The anisotropy ratio ρ_c/ρ_{ab} increases monotonically as a function of temperature from 160 at $T=300 \text{ K}$ to 850 at $T=0.3 \text{ K}$, which is similar to the ratios of pure Sr_2RuO_4 . At room temperature the in-plane resistivity (left scale) is enhanced by a factor of 2.5 when compared to the pure compound. On decreasing temperature ρ_{ab} decreases, passes through a minimum, and exhibits a semiconducting characteristic for $T < 40 \text{ K}$. This minimum could signal the onset of localization of charge carriers within the ab plane, Kondo-type scattering of charge carriers on localized moments, or a partial gapping of the Fermi surface due to the formation of a spin-density wave. We will see later that at 5 K the optical conductivity reveals a metallic Drude-type behavior. In addition we carefully analyzed the resistivity upturn for $x=0.2$ and $T < 50 \text{ K}$ in terms of a Kondo-like in-

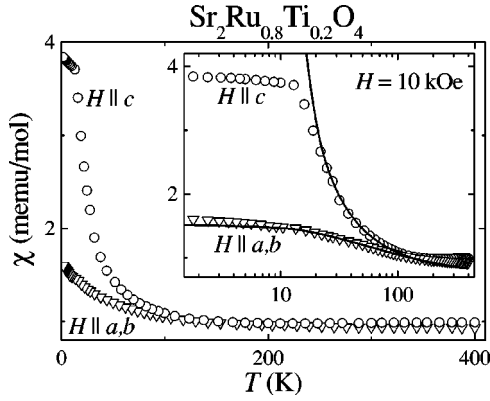


FIG. 2. Temperature dependence of the dc susceptibility in $\text{Sr}_2\text{Ru}_{0.8}\text{Ti}_{0.2}\text{O}_4$ measured with an applied field of 10 kOe parallel to the c axis (χ_c circles) and within the ab plane (χ_{ab} triangles). The inset shows $\chi_{ab}(T)$ and $\chi_c(T)$ in a semilogarithmic plot.

crease or hopping conductivity of localized charge carriers. Both models do not provide a reasonable description of the low-temperature upturn. Guided by these facts we prefer to interpret $\rho(T)$ for low temperatures by the onset of short-range magnetic order. The interlayer resistivity (right scale) reveals a semiconducting temperature variation for all temperatures investigated. For $T > 100$ K it is enhanced by a factor of 2 when compared to the undoped compound, but ρ_c never enters a metallic regime, which is observed for $x = 0$ at low temperatures.

B. Magnetic susceptibility and magnetization

As a representative result Fig. 2 shows the susceptibility for $\text{Sr}_2\text{Ru}_{0.8}\text{Ti}_{0.2}\text{O}_4$ as measured for an external dc field of 10 kOe. For $T > 100$ K we find an almost isotropic Pauli-spin susceptibility of approximately 10^{-3} emu/mol, very similar to the results obtained in undoped Sr_2RuO_4 (Refs. 26 and 30). This behavior demonstrates that at elevated temperatures Ti^{4+} ($3d^0$) replaces Ru^{4+} ($4d^4$) resulting in Fermi-liquid (FL) behavior without localized moments. From the temperature dependence of the resistivity (Fig. 1) it seems clear that the FL has quasi-two-dimensional (2D) character as expected from the crystallographic structure. However, below 100 K a Curie-Weiss-like behavior evolves and concomitantly a strong magnetic anisotropy appears, with the c -axis susceptibility χ_c strongly enhanced compared to the in-plane susceptibility χ_{ab} . This is also true for $x = 0.1$. The results look similar to those reported by Minakata and Maeno.²⁶ An apparent Curie-Weiss (CW) law for $T < 150$ K is followed by a nearly temperature-independent isotropic Pauli-like behavior at elevated temperatures.

We attempted to fit $\chi(T)$ using the sum of a temperature-independent Pauli-spin susceptibility χ_{Pauli} and a CW contribution,

$$\chi(T) = \chi_{\text{Pauli}} + \frac{A}{T - \Theta}. \quad (1)$$

At elevated temperatures the Pauli-spin susceptibility contribution is enlarged compared to the contribution of the local-

TABLE II. Parameters as determined by the fits of Eq. (1) to the magnetic susceptibility of $\text{Sr}_2\text{Ru}_{1-x}\text{Ti}_x\text{O}_4$.

Ti concentration	$x = 0.1$		$x = 0.2$	
$H \parallel$	a, b	c	a, b	c
χ_{Pauli} (emu/mol)	6×10^{-4}	6×10^{-4}	7×10^{-4}	7×10^{-4}
μ_{eff} ($\mu_B/\text{f.u.}$)	0.73	0.47	0.65	0.50
Θ (K)	-100	2.5	-58	5.8

ized moments. Therefore no clear prediction is possible if either the localized moments are still existing, but are hard to detect, or the localized moments disappear. The best-fit results are indicated as solid lines in the inset of Fig. 2, which shows χ_c and χ_{ab} vs T on a semilogarithmic plot to demonstrate the quality of the fit. The corresponding values for the effective paramagnetic moment μ_{eff} , the CW temperature Θ , and the Pauli contribution χ_{Pauli} are given in Table II. Certainly the fit of Eq. (1) to $\chi(T)$ is not convincing at high temperatures. This is due to the fact that for $T > 100$ K $\chi(T)$ slightly increases on increasing temperature. It is this behavior which led Neumeier *et al.*³¹ to add a term which is linear in T . It is worth mentioning that the data can be well fitted in the complete range up to room temperature employing this additional linear term $\chi_{\text{cor}}T$ without having significant influence on the results for the parameters χ_{Pauli} , μ_{eff} , and Θ .

An alternative interpretation for the deviation from Pauli behavior at elevated temperatures rests on the assumption that for $T > 100$ K, $\text{Sr}_2\text{Ru}_{1-x}\text{Ti}_x\text{O}_4$ behaves like a 2D anti-ferromagnet with a large exchange constant. In these systems the exchange corresponds to a maximum in the susceptibility which then would be expected at $T > 400$ K and thereby the increasing susceptibility with increasing temperature can be well described. Similar observations have been reported for low-doped $\text{La}_{2-x}\text{Sr}_x\text{CuO}_4$ (Ref. 32).

A parametrization of the data using Eq. (1) gives strong AFM correlations within the ab plane ($\Theta \approx -100$ K) and an almost pure Curie behavior along c ($\Theta \approx 0$ K), indicating that the local moments are almost decoupled perpendicular to the c axis. Taking this model seriously $\text{Sr}_2\text{Ru}_{1-x}\text{Ti}_x\text{O}_4$ has to be characterized as a 2D magnet with a strong in-plane coupling.

For the c direction the values of the paramagnetic moment $\mu_{\text{eff}} \approx 0.5 \mu_B/\text{f.u.}$ are larger than the values found by Minakata and Maeno.²⁶ The paramagnetic moments for the ab plane are enhanced compared to the c axis. Thus the in-plane magnetic properties of the Ti-doped compounds seem to reflect the properties of pure Sr_2RuO_4 , where values of $\mu_{\text{eff}} \approx 1 \mu_B$ and $\Theta \approx -150$ K were reported.³¹

Figure 3 displays the temperature dependence of the magnetization for lower temperatures for both Ti concentrations. A clear splitting of the field-cooled (FC) and zero-field-cooled (ZFC) magnetizations occurs close to $T_m = 15$ K for $H \parallel c$. Only minor effects show up for the in-plane magnetization which might result from a slight misalignment of the sample. T_m is in agreement with the phase diagram published by Minakata and Maeno,²⁶ which shows a saturation of T_m for Ti concentration $x > 0.12$. The fact that for $x = 0.1$ and 0.2

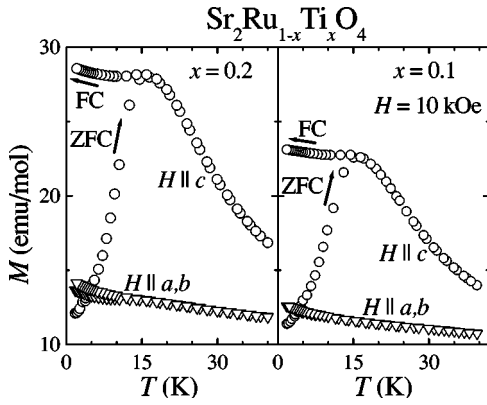


FIG. 3. Magnetization vs temperature for $\text{Sr}_2\text{Ru}_{1-x}\text{Ti}_x\text{O}_4$ for $x=0.1$ (right panel) and $x=0.2$ (left panel) for an external field of 10 kOe with $H\parallel c$ and $H\parallel a,b$. FC and ZFC cycles are shown.

the characteristic temperatures T_m are almost the same could indicate slight deviations of the effective Ti concentration from the nominal composition.

One is tempted to assume spin-glass-like ordering of statistically substituted local $3d^1$ states embedded in a Fermi liquid of the band states. However, the FC and ZFC cycles were performed at relatively high fields of 10 kOe. At such high fields spin-glass effects often are suppressed.³³ The FC and ZFC splittings can also indicate the formation of FM clusters or even true long-range ferromagnetism were the FC and ZFC splitting results from domain-wall effects in strongly anisotropic materials. Having the time dependence of magnetization in mind, which has been observed by Minakata and Maeno,²⁶ it seems most plausible to assume short-range FM correlations only. We also would like to stress that magnetization for fields within the ab plane is not affected at all and for low temperatures the zero-field curve with $H\parallel c$ is well below M with $H\parallel a,b$. So the observed magnetic transition is due to a coupling of the moments along c only.

Figure 4 shows the magnetization vs an external magnetic field below the magnetic ordering temperature (lower frame: $T=5$ K, upper frame: $T=13$ K). At both temperatures the in-plane magnetization M_{ab} behaves like a purely paramagnetic compound (or an AFM compound well below a spin-flop field). However, with the applied field along c a clear FM hysteresis evolves. The coercitive fields rapidly increase towards lower temperatures. At 5 K the maximum applied field of 50 kOe is already much too small to establish a complete alignment of the spins. The ordered moment is rather low, and of the order of $0.01\mu_B/\text{f.u.}$

C. Heat capacity

Figure 5 shows the low-temperature heat capacity C for $\text{Sr}_2\text{Ru}_{1-x}\text{Ti}_x\text{O}_4$ for $x=0.1$ and 0.2 , plotted as C/T vs T . With increasing x the low-temperature plateau, which so far has been interpreted as a strongly enhanced Sommerfeld coefficient γ , becomes suppressed. γ is $40 \text{ mJ mol}^{-1}\text{K}^{-2}$ in the pure compound^{11,12,31} and becomes reduced to values of approximately $27 \text{ mJ mol}^{-1}\text{K}^{-2}$ ($23 \text{ mJ mol}^{-1}\text{K}^{-2}$) for $x=0.1$ (0.2). A hyperfine term appears at low temperatures.

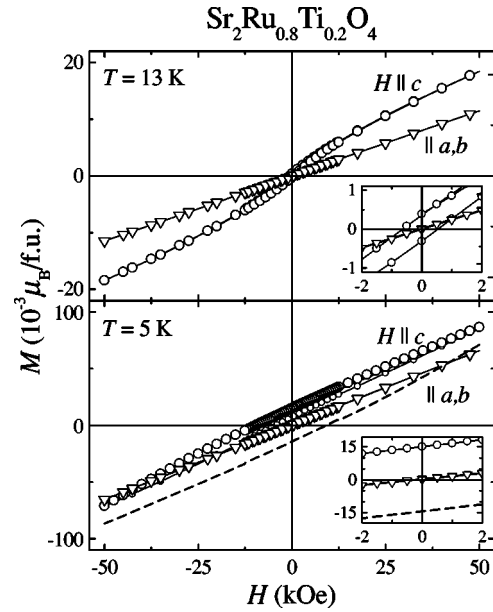


FIG. 4. Magnetization vs applied field for $\text{Sr}_2\text{Ru}_{0.8}\text{Ti}_{0.2}\text{O}_4$ at $T=13$ K (upper panel) and $T=5$ K (lower panel). Magnetizations within the ab plane (M_{ab} , triangles) and c direction (M_c , circles) are shown. The dashed line is a mirror image of the measured M_{ab} data.

We have calculated the hyperfine contributions to the heat capacity resulting from ^{87}Sr , ^{99}Ru , and ^{101}Ru , assuming an average magnetic field and Zeeman splitting. We can fit the low-temperature upturn assuming a local field of approximately 850 kOe. The local field seems very strong but still could be reasonable, e.g., in $\text{La}_{0.8}\text{Sr}_{0.2}\text{MnO}_3$ local fields about 390 kOe were detected.³⁴ But these strong internal fields can be only explained by strong FM correlations and probably point towards short-range FM order at least. The same fitting procedure for increasing external fields yields increasing internal fields and for $H=100$ kOe we found an internal field of approximately 1250 kOe. The inset in Fig. 5 shows the Schottky-like increase towards low temperatures as a function of an external magnetic field. Fields signifi-

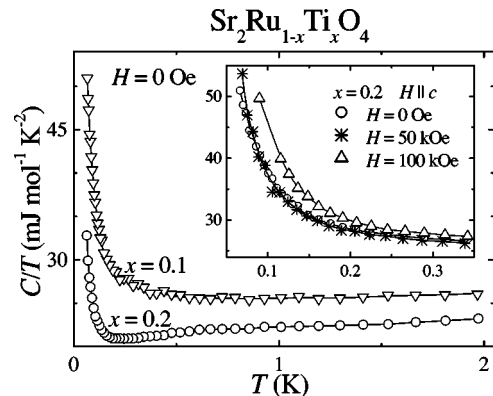


FIG. 5. Heat capacity C/T vs T in $\text{Sr}_2\text{Ru}_{1-x}\text{Ti}_x\text{O}_4$ for $x=0.1$ (triangles) and $x=0.2$ (circles) at zero external field. The inset shows the temperature dependence of C/T for external magnetic fields up to 100 kOe. All solid lines are drawn to guide the eye.

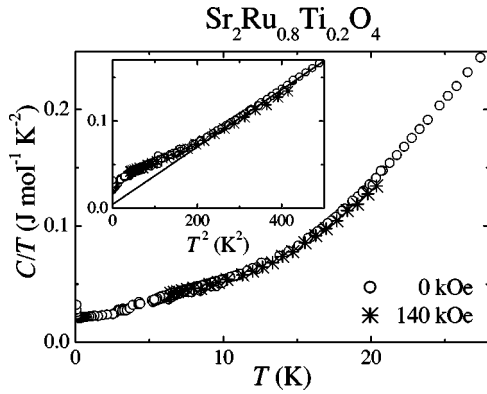


FIG. 6. Heat capacity C/T vs T for $\text{Sr}_2\text{Ru}_{0.8}\text{Ti}_{0.2}\text{O}_4$ in zero external field (circles) and for fields of 140 kOe (crosses). The inset shows the same data as C/T vs T^2 . The solid line is an extrapolation of the lattice contribution towards low temperatures.

cantly higher than 50 kOe are necessary to enhance the hyperfine term. This observation is compatible with the extremely high saturation magnetization which is indicated in Fig. 4.

Figure 6 shows C/T vs T for $\text{Sr}_2\text{Ru}_{0.8}\text{Ti}_{0.2}\text{O}_4$ for temperatures $0.1 \text{ K} < T < 30 \text{ K}$, in zero external field (circles) and in a magnetic field of 140 kOe (crosses). C/T smoothly increases with no anomaly, specifically not close to 15 K where the anomaly in the out-of-plane magnetization has been detected. For temperatures $T > 5 \text{ K}$, C/T reveals no field dependence up to 140 kOe. In spin glasses a cusp would be expected at $T \approx 1.3 T_g$, which in our case should occur close to 20 K. At the onset of long-range magnetic order an anomaly at $T_m = 15 \text{ K}$ should show up. Neither anomaly can be detected in Fig. 6. The fact that a heat-capacity anomaly is missing favors an interpretation in terms of cluster ferromagnetism or spin-glass freezing. The inset shows C/T vs T^2 and analyzing the heat capacity for $15 \text{ K} < T < 25 \text{ K}$ a Sommerfeld coefficient of the order of $15 \text{ mJ mol}^{-1}\text{K}^{-2}$ (solid line) can be determined. Close to 15 K additional contributions to the heat capacity show up, which most probably are magnetic in origin. We would like to mention that a similar analysis could be performed using the published data for Sr_2RuO_4 (Ref. 31) and would result in a much lower Sommerfeld coefficient. Based on our results we suggest that C/T at low temperatures is due to spin fluctuations even in the pure compound.

D. Optical conductivity

We have investigated the reflectivity R of $\text{Sr}_2\text{Ru}_{0.8}\text{Ti}_{0.2}\text{O}_4$ in the range of wave numbers λ^{-1} from 50 to $33\,000 \text{ cm}^{-1}$. Due to the sample geometry, reflectivity measurements with $E \parallel c$ could only be performed using an IR microscope, which operates in the mid-infrared (MIR) range ($700 \text{ cm}^{-1} < \lambda^{-1} < 7000 \text{ cm}^{-1}$) only.

The E direction and frequency dependence of the reflectivity at MIR frequencies for the ac direction of $\text{Sr}_2\text{Ru}_{0.8}\text{Ti}_{0.2}\text{O}_4$ is shown in Fig. 7. The most striking result is the extreme anisotropy of the charge dynamics which is nicely documented. The reflectivity reveals a typical insulat-

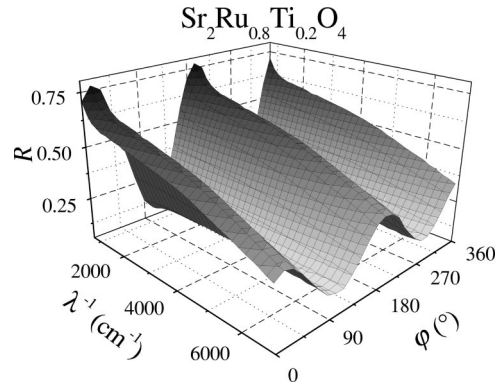


FIG. 7. MIR reflectivity vs wave number and direction of E within the ac plane for $\text{Sr}_2\text{Ru}_{0.8}\text{Ti}_{0.2}\text{O}_4$.

ing behavior in the c direction ($\varphi \approx 110^\circ, 300^\circ$) with nearly constant $R \approx 0.16$. In the ab direction ($\varphi \approx 20^\circ, 210^\circ$) the reflectivity is much higher ($R \approx 0.78$ at 700 cm^{-1}) and decreases with increasing wave number.

Figure 8 shows the in-plane reflectivity in a broad frequency range and the out-of-plane MIR reflectivity for $x = 0.2$ (solid lines). The MIR reflectivity for $x = 0.1$ (dotted lines) is also shown. The in-plane reflectivity of $\text{Sr}_2\text{Ru}_{0.8}\text{Ti}_{0.2}\text{O}_4$ decreases with increasing temperature in a Drude-like fashion, similar to observations in pure Sr_2RuO_4 (Ref. 35). The out-of-plane reflectivity resembles the data of the pure compound, being quite different from the in-plane R . It is nearly frequency independent at $1500 \text{ cm}^{-1} < \lambda^{-1} < 7000 \text{ cm}^{-1}$ and shows no Drude-like behavior in the measured frequency range. Due to the sample size for $x = 0.1$ (dotted lines) only the MIR reflectivity could be measured. R is enhanced in- and out-of-plane compared to $x = 0.2$, but still is smaller than the values of the undoped compound.³⁵ This can be interpreted as a reduction of free charge carriers with increasing Ti doping.

In order to investigate the optical conductivity, a Kramers-Kronig analysis of the reflectivity was carried out for $x = 0.2$ at $T = 5 \text{ K}$ and $T = 300 \text{ K}$. For the low-frequency extrapolation the Hagen-Rubens formula has been assumed.

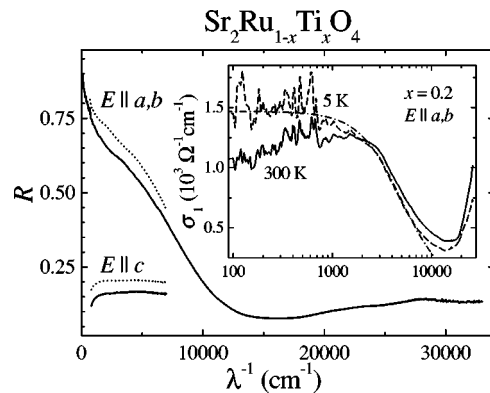


FIG. 8. In-plane and out-of-plane reflectivities for $x = 0.2$ (solid lines) and $x = 0.1$ (dotted lines) at $T = 300 \text{ K}$. Inset: Real part of optical conductivity for $\text{Sr}_2\text{Ru}_{0.8}\text{Ti}_{0.2}\text{O}_4$ at $T = 5 \text{ K}$ (dashed line), $T = 300 \text{ K}$ (solid line), and a Drude fit for $T = 5 \text{ K}$ (dash-dotted line).

The real part of the optical conductivity $\sigma_1(\omega)$ is shown for $T=5$ K (dashed line) and $T=300$ K (solid line) in the inset of Fig. 8. The peaklike structures below 1000 cm^{-1} result from weak reminders of the phonon peaks and from multiple-scattering events of the light passing the cryostat windows. Turning first to the room-temperature spectra, both the reflectivity and optical conductivity for $\text{Sr}_2\text{Ru}_{0.8}\text{Ti}_{0.2}\text{O}_4$ are very similar to those observed in the related cuprates $\text{La}_{2-y}\text{Sr}_y\text{CuO}_4$ (Ref. 36). In the cuprates the optical spectra for $y=0.06$ and $y=0.1$ are very close in the absolute values and shape to what is observed in the ruthenates under investigation. The slight non-Drude response towards low frequencies, namely, a bump that is observed close to 2000 cm^{-1} (see inset in Fig. 8) is also a characteristic feature of many low-doped cuprates. This bump could be disorder induced and probably is a characteristic feature for metals close to localization. The fact that the conductivity spectrum for $x=0.2$ at room temperature is close to the spectra observed in $\text{La}_{1.9}\text{Sr}_{0.1}\text{CuO}_4$ is a further hint for the extremely low charge-carrier concentration of the titanium-doped ruthenates.

To compare the effective number of charge carriers N_{eff} in the ab plane with the pure Sr_2RuO_4 we calculated the spectral weight for the 20% Ti-doped sample up to $12\,000$ cm^{-1} (≈ 1.5 eV). N_{eff} is given by

$$N_{eff}(\omega) = \frac{2m_0}{Ne^2\pi} \int_0^\omega \sigma_1(\omega') d\omega', \quad (2)$$

where m_0 is the free-electron mass, e is the elementary charge, and N is the number of Ru and Ti atoms per unit volume. We find $N_{eff}^{300\text{K}}$ (per formula unit) = 0.38 at room temperature, which is clearly reduced when compared to $N_{eff}^{290\text{K}} = 0.53$ as observed in the pure compound.³⁵ On the other hand, if N is taken as the number of Ru atoms per unit volume, we get a value of $N_{eff}^{300\text{K}}(\text{Ru}) = 0.48$ which is close to that of pure Sr_2RuO_4 . At 5 K the effective number of electrons is only slightly reduced to $N_{eff}^{5\text{K}}$ (per formula unit) = 0.36, however the dc conductivity at 5 K is clearly enhanced compared to 300 K. A shift of the spectral weight towards high frequencies often is observed in highly correlated electron systems. It also is clear that at 5 K the optical conductivity is close to a Drude-like behavior which contradicts the observation in the dc resistivity where localization effects were detected at low temperatures.

We fitted the real part of conductivity with a standard Drude model in order to estimate the plasma frequency ω_p and the scattering rate γ using

$$\sigma_1(\omega) = \frac{\varepsilon_0 \omega_p^2 \gamma}{\gamma^2 + \omega^2}, \quad (3)$$

where ε_0 is the dielectric constant of vacuum. At $T=5$ K Eq. (3) provides a good fit to the data (dash-dotted line in the inset of Fig. 8). We find a plasma frequency $\omega_p^{5\text{K}} = 20\,947$ cm^{-1} and a scattering rate $\gamma^{5\text{K}} = 4958$ cm^{-1} . At room temperature $\sigma_1(\omega)$ looks rather similar, with the scattering rate $\gamma^{300\text{K}} = 6465$ cm^{-1} and the plasma frequency $\omega_p^{300\text{K}} = 22\,197$ cm^{-1} being slightly increased. $\sigma_1^{\text{Drude}}(\omega \rightarrow 0)$

= 1475 $\Omega^{-1} \text{cm}^{-1}$ and $\sigma_1^{300\text{K}}(\omega \rightarrow 0) = 1270$ $\Omega^{-1} \text{cm}^{-1}$ are in rough agreement with the dc conductivity shown in Fig. 1.

IV. SUMMARY AND CONCLUSIONS

In this work we investigated single crystals of $\text{Sr}_2\text{Ru}_{1-x}\text{Ti}_x\text{O}_4$ with concentrations of $x=0.1$ and 0.2 which were grown using the floating-zone melting technique. The crystals show an anisotropic behavior of dc resistivity and infrared reflectivity similar to that observed in undoped Sr_2RuO_4 , but the temperature dependence of dc resistivity is rather different. The resistivity along c reveals a semiconducting behavior down to the lowest temperatures and the resistivity within the RuO_2 planes signals the onset of localization effects close to 50 K. From the magnetic susceptibility and the magnetization we conclude that the crystals exhibit an anisotropic Curie-Weiss behavior at temperatures below 100 K. Moreover magnetic ordering along c with a moment of order $0.01\mu_B/\text{f.u.}$ evolves at $T < 15$ K. At the moment it is unclear if long-range or short-range magnetism is established below T_m . However it is clear that strong AFM exchange dominates the in-plane properties while FM coupling between the planes establishes FM correlations along c . Antiferromagnetic order within the planes corresponds to spin arrangements observed in La_2CuO_4 and La_2NiO_4 and also were detected in Ca_2RuO_4 (Ref. 37). We also speculate that even at elevated temperatures the Ti-doped ruthenates behave like two-dimensional magnets similar to what has been observed in Sr-doped La_2CuO_4 (Ref. 32). High-temperature susceptibility measurements, even in the pure compound, are highly warranted. From the heat-capacity experiments we find that the Sommerfeld coefficient significantly becomes suppressed on Ti doping reaching values of 27 $\text{mJ mol}^{-1}\text{K}^{-2}$ for $x=0.1$ and 23 $\text{mJ mol}^{-1}\text{K}^{-2}$ for $x=0.2$, which still are extremely high values for a bad metal close to localization with a low density of charge carriers. Carrying out the heat capacity in a broader temperature range, we find that just below the magnetic ordering transition the susceptibility becomes considerably enhanced and at low temperatures possibly soft magnetic excitations dominate the heat capacity. However, at the magnetic ordering temperature, as observed in the susceptibility experiments, no heat-capacity anomalies indicative of long-range magnetic order were detected. This can be interpreted as additional evidence that only short-range order exists below T_m . It is interesting to note that the heat capacity for $T > 1$ K remains unchanged in fields as high as 140 kOe.

The reflectivity shows an anisotropic behavior of the charge dynamics similar to the parent compound. The in- and out-of-plane reflectivities decrease in the complete frequency range investigated with increasing Ti doping. The frequency dependencies of the reflectivity and the conductivity are similar to the low-doped regime of $\text{La}_{2-y}\text{Sr}_y\text{CuO}_4$ ($y \approx 0.06$). We fit the in plane $\sigma_1(\omega)$ using a standard Drude model, which describes the experimental results well at $T = 5$ K. At this temperature, the plasma frequency is approximately 2.3 eV, and the scattering rate is of the order of 0.6 eV. Both quantities increase on increasing temperature. We

also tried to calculate the optical weight of the Drude response and found an effective number of charge carriers of 0.38 (per formula unit at 300 K), assuming that both Ru and Ti atoms contribute to the band states. This value is significantly reduced when compared to the number of charge carriers in the pure system ($N_{eff}=0.53$) as determined by Katsufuji *et al.*³⁵

ACKNOWLEDGMENTS

The authors gratefully acknowledge enlightening conversations with Christoph Langhammer. This work was partly supported by the DFG via the Sonderforschungsbereich 484 (Augsburg) and Project No. Eb 219/1-1, and partly by the BMBF via Contract No. EKM/13N6917/0.

- ¹J.J. Randall and R. Ward, *J. Am. Chem. Soc.* **81**, 2629 (1959).
- ²Y. Maeno, H. Hashimoto, K. Yoshida, S. Nishizaki, T. Fujita, J.G. Bednorz, and F. Lichtenberg, *Nature (London)* **372**, 532 (1994).
- ³A.P. Mackenzie, R.K.W. Haselwimmer, A.W. Tyler, G.G. Lonzarich, Y. Mori, S. Nishizaki, and Y. Maeno, *Phys. Rev. Lett.* **80**, 161 (1998).
- ⁴Z.Q. Mao, Y. Mori, and Y. Maeno, *Phys. Rev. B* **60**, 610 (1999).
- ⁵T.M. Rice and M. Sigrist, *J. Phys.: Condens. Matter* **7**, L643 (1995).
- ⁶M. Sigrist, D. Agterberg, A. Furusaki, C. Honerkamp, K.K. Ng, T.M. Rice, and M.E. Zhitomirsky, *Physica C* **317-318**, 134 (1999).
- ⁷G. Baskaran, *Physica B* **223-224**, 490 (1996).
- ⁸K. Ishida, H. Mukuda, Y. Kitaoka, K. Asayama, Z.Q. Mao, Y. Mori, and Y. Maeno, *Nature (London)* **396**, 658 (1998).
- ⁹G.M. Luke, Y. Fudamoto, K.M. Kojima, M.I. Larkin, J. Merrin, B. Nachumi, Y.J. Uemura, Y. Maeno, Z.Q. Mao, Y. Mori, H. Nakamura, and M. Sigrist, *Nature (London)* **394**, 558 (1998).
- ¹⁰P.G. Kealey, T.M. Riseman, E.M. Forgan, L.M. Galvin, A.P. Mackenzie, S.L. Lee, D.M. Paul, R. Cubitt, D.F. Agterberg, R. Heeb, Z.Q. Mao, and Y. Maeno, *Phys. Rev. Lett.* **84**, 6094 (2000).
- ¹¹S. Nishizaki, Y. Maeno, and Z. Mao, *J. Low Temp. Phys.* **117**, 1581 (1999).
- ¹²S. Nishizaki, Y. Maeno, S. Farmer, S. Ikeda, and T. Fujita, *Physica C* **282-287**, 1413 (1997).
- ¹³K. Ishida, H. Mukuda, Y. Kitaoka, Z.Q. Mao, Y. Mori, and Y. Maeno, *Phys. Rev. Lett.* **84**, 5387 (2000).
- ¹⁴A. Kanbayasi, *J. Phys. Soc. Jpn.* **44**, 108 (1976).
- ¹⁵S.I. Ikeda, Y. Maeno, S. Nakatsuji, M. Kosaka, and Y. Uwatoko, *Phys. Rev. B* **62**, R6089 (2000).
- ¹⁶Y. Sidis, M. Braden, P. Bourges, B. Hennion, S. Nishizaki, Y. Maeno, and Y. Mori, *Phys. Rev. Lett.* **83**, 3320 (1999).
- ¹⁷H. Mukuda, K. Ishida, Y. Kitaoka, K. Asayama, Z. Mao, Y. Mori, and Y. Maeno, *J. Phys. Soc. Jpn.* **67**, 3945 (1998).
- ¹⁸H. Mukuda, K. Ishida, Y. Kitaoka, K. Asayama, R. Kanno, and M. Takano, *Phys. Rev. B* **60**, 12 279 (1999).
- ¹⁹T. Imai, A.W. Hunt, K.R. Thurber, and F.C. Chou, *Phys. Rev. Lett.* **81**, 3006 (1998).
- ²⁰I.I. Mazin and D.J. Singh, *Phys. Rev. Lett.* **82**, 4324 (1999).
- ²¹T. Kuwabara and M. Ogata, *Phys. Rev. Lett.* **85**, 4586 (2000).
- ²²G. Cao, S. McCall, M. Shepard, J.E. Crow, and R.P. Guertin, *Phys. Rev. B* **56**, R2916 (1997).
- ²³R.J. Cava, B. Batlogg, K. Kiyono, H. Takagi, J.J. Krajewski, W.F. Peck, Jr., L.W. Rupp, Jr., and C.H. Chen, *Phys. Rev. B* **49**, 11 890 (1994).
- ²⁴S.A. Carter, B. Batlogg, R.J. Cava, J.J. Krajewski, W.F. Peck, Jr., and L.W. Rupp, Jr., *Phys. Rev. B* **51**, 17 184 (1995).
- ²⁵H.R. Oswald, S. Felder-Casagrande, and A. Reller, *Solid State Ionics* **63-65**, 565 (1993).
- ²⁶M. Minakata and Y. Maeno, *Phys. Rev. B* **63**, 180504(R) (2001).
- ²⁷H.C. Montgomery, *J. Appl. Phys.* **42**, 2971 (1971).
- ²⁸H.R. Ott, H. Rudigier, Z. Fisk, and J.L. Smith, *Phys. Rev. B* **31**, 1651 (1985).
- ²⁹F. Lichtenberg, A. Catana, J. Mannhart, and D.G. Schlom, *Appl. Phys. Lett.* **60**, 1138 (1992).
- ³⁰Y. Maeno, K. Yoshida, H. Hashimoto, S. Nishizaki, S. Ikeda, M. Nohara, T. Fujita, A.P. Mackenzie, N.E. Hussey, J.G. Bednorz, and F. Lichtenberg, *J. Phys. Soc. Jpn.* **66**, 1405 (1997).
- ³¹J.J. Neumeier, M.F. Hundley, M.G. Smith, J.D. Thompson, C. Allgeier, H. Xie, W. Yelon, and J.S. Kim, *Phys. Rev. B* **50**, 17 910 (1994).
- ³²D.C. Johnston, *Phys. Rev. Lett.* **62**, 957 (1989).
- ³³J. A. Mydosh, *Spin Glasses: An Experimental Introduction* (Taylor & Francis, London, 1993).
- ³⁴B.F. Woodfield, M.L. Wilson, and J.M. Byers, *Phys. Rev. Lett.* **78**, 3201 (1997).
- ³⁵T. Katsufuji, M. Kasai, and Y. Tokura, *Phys. Rev. Lett.* **76**, 126 (1996).
- ³⁶S. Uchida, T. Ido, H. Takagi, T. Arima, Y. Tokura, and S. Tajima, *Phys. Rev. B* **43**, 7942 (1991).
- ³⁷M. Braden, G. Andre, S. Nakatsuji, and Y. Maeno, *Phys. Rev. B* **58**, 847 (1998).